Enantioselective Potassium-Catalyzed Wittig Olefinations

Jake Z. Essman and Eric N. Jacobsen*

Department of Chemistry and Chemical Biology, Harvard University, Cambridge, MA 02138, USA.

ABSTRACT: We report asymmetric potassium-isothiourea-boronate–catalyzed Wittig olefinations of 4-substituted cyclohexanones with non-stabilized phosphorus ylides to afford highly enantioenriched axially chiral alkenes. The optimal catalyst features an unusual macrocyclic amide-potassium-boronate chelate. Kinetic and spectroscopic analyses are consistent with a Lewis acid mechanism for the catalytic olefination that results in formation of the oxaphosphetane adduct under cryogenic conditions. Thermal fragmentation of the oxaphosphetane to the alkene product occurs after the reaction is complete. Computational studies indicate that cycloaddition proceeds via a stepwise mechanism involving enantiodetermining polar 1,2-addition to afford an intermediate potassium betaine complex.

The Wittig reaction has stood as one of the essential methods for stereoselective alkene synthesis since its initial report,[1,2] finding continuous application in both industry and academia to this day.[3–7] Olefination of suitably substituted prochiral ketones permits the formation of axially chiral alkene products,[8–13] and numerous approaches to asymmetric Wittig and Horner–Wadsworth–Emmons reactions have been demonstrated using stoichiometric chiral controlling elements,[14] with canonical examples relying on covalent chiral auxiliaries[15–17] or chiral ligands.[18,19] In contrast, examples of asymmetric catalysis of Wittig-type olefinations to access axially chiral products are exceedingly rare; to our knowledge there exist only three reported examples, using either Brønsted acid, H-bond-donor, or phase-transfer catalysts and attaining up to 75% enantiomeric excess (ee) (Scheme 1A).[20–23] Herein, we report highly enantioselective Wittig reactions of 4-substituted cyclohexanones catalyzed by a novel potassium-isothiourea-boronate complex.

The generally accepted mechanism for the Wittig reaction involves an initial irreversible asynchronous concerted [2+2] cycloaddition between a carbonyl compound and a phosphorus ylide to form a mixture of *cis*- and *trans*-oxaphosphetane (OPA) species, followed by an irreversible stereospecific cycloreversion to afford the corresponding alkene and phosphine oxide (Scheme 1B).[24–27] Zwitterionic "salt-free" betaine species have not been observed during Wittig reactions, and have been conclusively excluded as possible intermediates in the reactions of certain classes of ylides.[28] However, Lewis acidic metal cations (typically Li^+) have been shown to stabilize betaine species and thereby influence the outcomes of Wittig olefinations.[29–32] Reactions of aldehydes with non-stabilized ylides exhibit a substantial decrease in *Z*-selectivity upon addition of lithium salts, consistent with the establishment of a lithium-mediated cycloaddition pathway via a betaine intermediate with lower kinetic selectivity for the formation of the *cis*-OPA (Scheme 1C).[24,29,33,34] Additionally, reactions of ketones with stabilized ylides are accelerated dramatically in the presence of lithium salts.[35]

Recently, our group discovered novel chiral lithium-isothiourea-boronate derivatives that catalyze highly enantioselective Matteson homologation reactions (Scheme 1D).[36,37] Given the observed effects of lithium salts on the rate and stereoselectivity of standard Wittig reactions, we considered whether this new family of chiral Lewis acids might exert enantiocontrol over Wittig reactions generating axially chiral alkenes. In particular, we envisioned that chiral alkali metal-based Lewis acids might catalyze the addition of non-stabilized phosphorus ylides to 4-substituted cyclohexanones to generate enantioenriched OPA intermediates (Scheme 1E). The resulting intermediate could then undergo stereospecific cycloreversion on warming to afford an enantioenriched axially chiral alkene product. Key to this strategy is the low-temperature stability of OPAs derived from non-stabilized ylides,[25,29] as the Lewis basic phosphine oxide byproduct of fragmentation to the alkene would likely be a potent catalyst poison.[38–40]

A preliminary assay of alkali metal-isothiourea-boronate derivatives developed in our study of the Matteson reaction revealed that while lithium- and sodium-based catalysts **Li-3a** and **Na-3a** afforded only racemic product in the olefination of 4-phenylcyclohexanone with ylide **2a**, the potassium-isothiourea-boronate derivative **K-3a** catalyzed the model reaction in 64% ee (Table 1). Reaction enantioselectivity proved highly responsive to the identity of the arylpyrrolidine moiety on the catalyst, with the unsubstituted derivative **K-3h** affording nearly racemic product and the 3-phenanthryl–substituted **K-3f**

Scheme 1. Synthetic and Mechanistic Aspects of Stereoselective Wittig Olefinations

A. Enantioselective catalytic Wittig and Horner–Wadsworth–Emmons reactions

Bestmann (1970), Arai (1998), Bernardi (2011): ***intermolecular****, to axially chiral alkene*

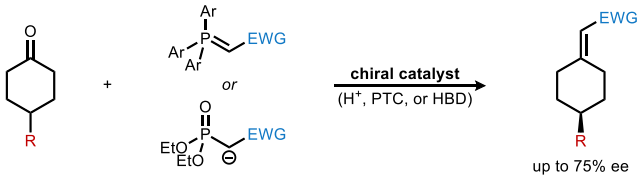

Werner (2014): ***intramolecular****, to bis-nor-Wieland–Miescher ketone*

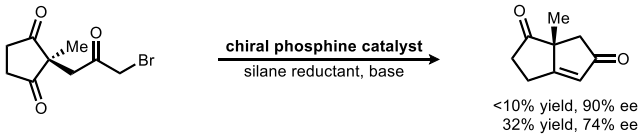

B. Mechanism of the Wittig olefination

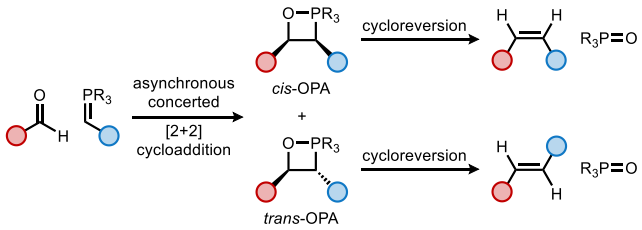

C. Lithium salt effects on stereoselectivity

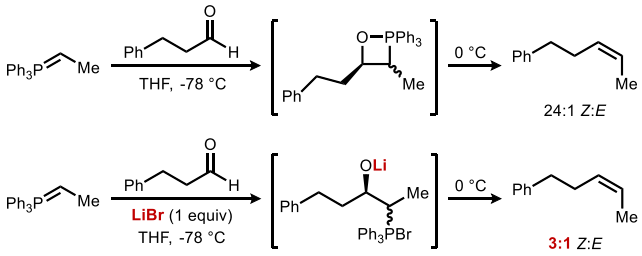

D. Enantioselective Li-isothiourea-boronate–catalyzed Matteson homologations

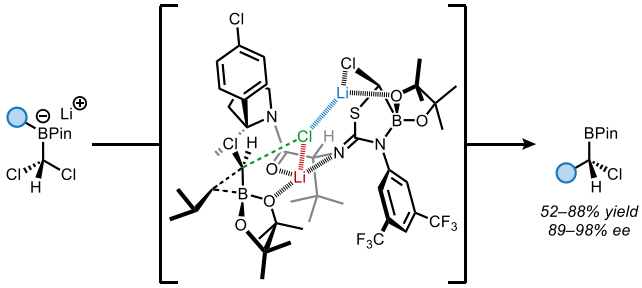

E. This work: Asymmetric metal-isothiourea-boronate–catalyzed Wittig reactions

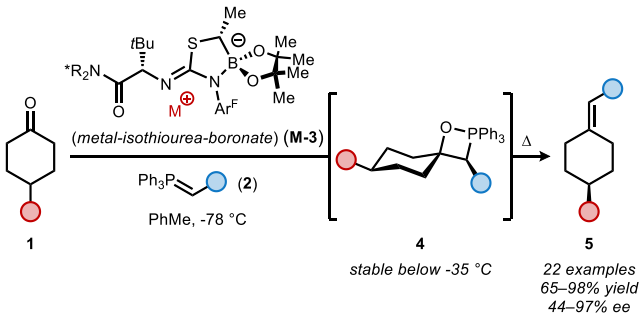

Table 1. Metal-Isothiourea-Boronate Catalyst Structure-Enantioselectivity Relationships

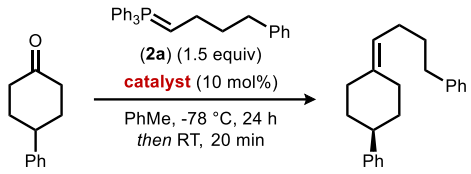

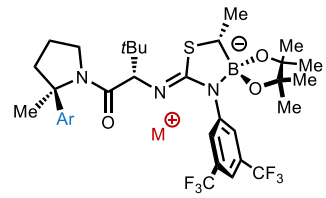

Li-3a (Ar = phenyl, M = Li): 0% ee

Na-3a (Ar = phenyl, M = Na): 0% ee

K-3a (Ar = phenyl, M = K): 64% ee

K-3b (Ar = 1-naphthyl): 39% ee

K-3c (Ar = 2-naphthyl): 87% ee

K-3d (Ar = 9-phenanthryl): 39% ee

K-3e (Ar = 2-phenanthryl): 48% ee

Li-3f (Ar = 3-phenanthryl): 0% ee

Na-3f (Ar = 3-phenanthryl): 30% ee

K-3f (Ar = 3-phenanthryl): **92% ee**

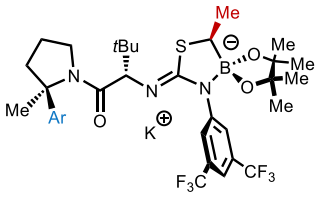

K-*epi*-3a (Ar = phenyl): 4% ee

K-*epi*-3b (Ar = 1-naphthyl): 1% ee

K-*epi*-3c (Ar = 2-naphthyl): 16% ee

K-*epi*-3d (Ar = 9-phenanthryl): -3% ee

K-*epi*-3e (Ar = 2-phenanthryl): 1% ee

K-*epi*-3f (Ar = 3-phenanthryl): 11% ee

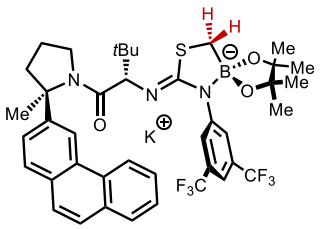

K-3g
90% ee

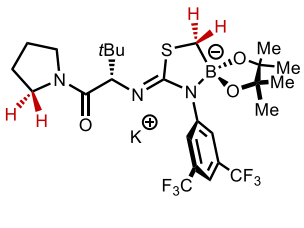

K-3h
2% ee

inducing the highest levels of selectivity (92% ee). The Na analog **Na-3f** was less enantioselective (30% ee), while the Li derivative afforded only racemic product. While removal of the α-boryl substituent had little effect on ee (**K-3g**, 90% ee), catalysts epimeric at the α-boryl stereocenter (**K-*epi*-3a–f**) promoted very poorly selective reactions in all cases.

We sought to elucidate the basis for the ligand effects and the superior performance of potassium-based catalysts in this transformation. An X-ray crystal structure analysis of **K-3f·THF** revealed an unusual macrocyclic chelate in which the potassium cation is coordinated between the amide oxygen and the anterior boronate oxygen (Figure 1A). This ligation mode is dramatically different from the five-membered amide-Li-isothiourea chelate previously observed in the X-ray structure of a lithium-isothiourea-boronate derivative.[36,37]

To assess the relevance of these solid-state structural differences to the corresponding solution structures, solution IR spectra of **M-3f** (M = Li, Na, K) were acquired and compared to spectra of the two chelates predicted by DFT (Figure 1B). The unmetallated

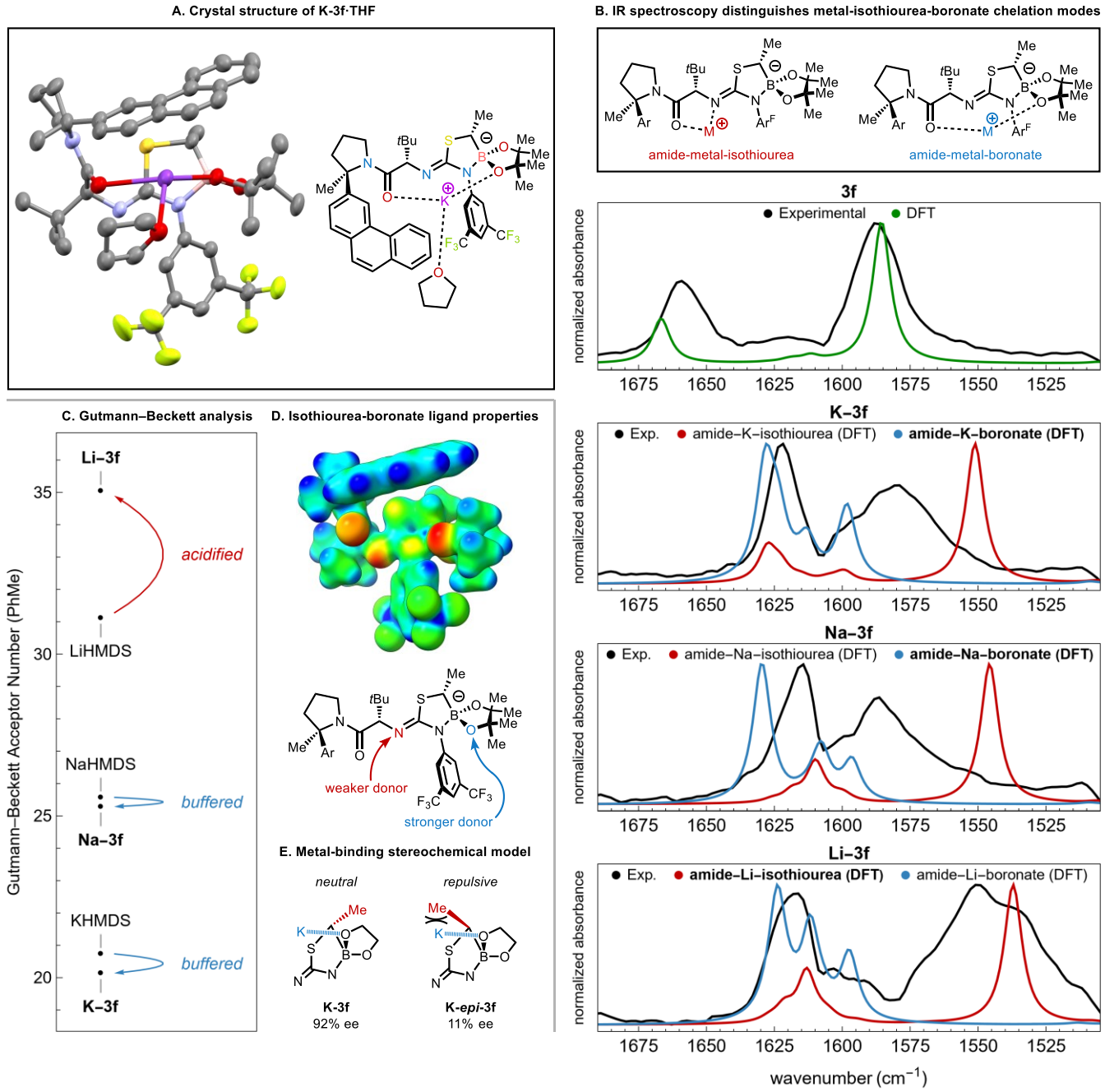

Figure 1. Characterization of alkali metal-isothiourea-boronate catalyst structures by (A) single-crystal X-ray diffraction; (B) IR spectroscopy; and (C) NMR studies. Hydrogen atoms and close contacts in the crystal structure of **K-3f·THF** are omitted for clarity. (D) Electrostatic potential map of anion derived from deprotonation of **3f**. Red = electron-rich, blue = electron-poor. (E) Proposed model of catalyst structure-enantioselectivity relationship.

isothiourea-boronate **3f** (M = H) exhibits absorbances corresponding to the amide C–O (1660 cm^{-1}) and isothiourea N–C–N (1590 cm^{-1}) moieties that are closely reproduced in the calculated spectrum. The spectra of **K-3f** and **Na-3f** display similar patterns in the carbonyl region, with a redshift of the C–O stretch by roughly 40 cm^{-1} and a flattening of the N–C–N stretch relative to the spectrum of **3f**. These spectral changes are in good agreement with predicted IR spectra of the amide-metal-boronate chelates. In contrast, the spectrum of **Li-3f** reveals a redshift of *both* peaks by roughly 40 cm^{-1}, in good agreement with the calculated amide-metal-isothiourea chelate (for in-depth discussion of IR spectra, see SI).[36,37]

These fundamental differences in chelation mode were found to translate into differences in relative Lewis acidity, as demonstrated in a Gutmann–Beckett analysis[38,39] (Figure 1C). A slight tempering of the Lewis acidity of **K-3f** relative to KHMDS and of **Na-3f** relative to NaHMDS is observed, whereas a significant increase in Lewis acidity is measured for **Li-3f** relative to LiHMDS. In an electrostatic potential map of the **3f**-derived isothiourea-boronate anion (Figure 1D), a high degree of electron density appears at the boronate oxygen atoms, consistent with the observed

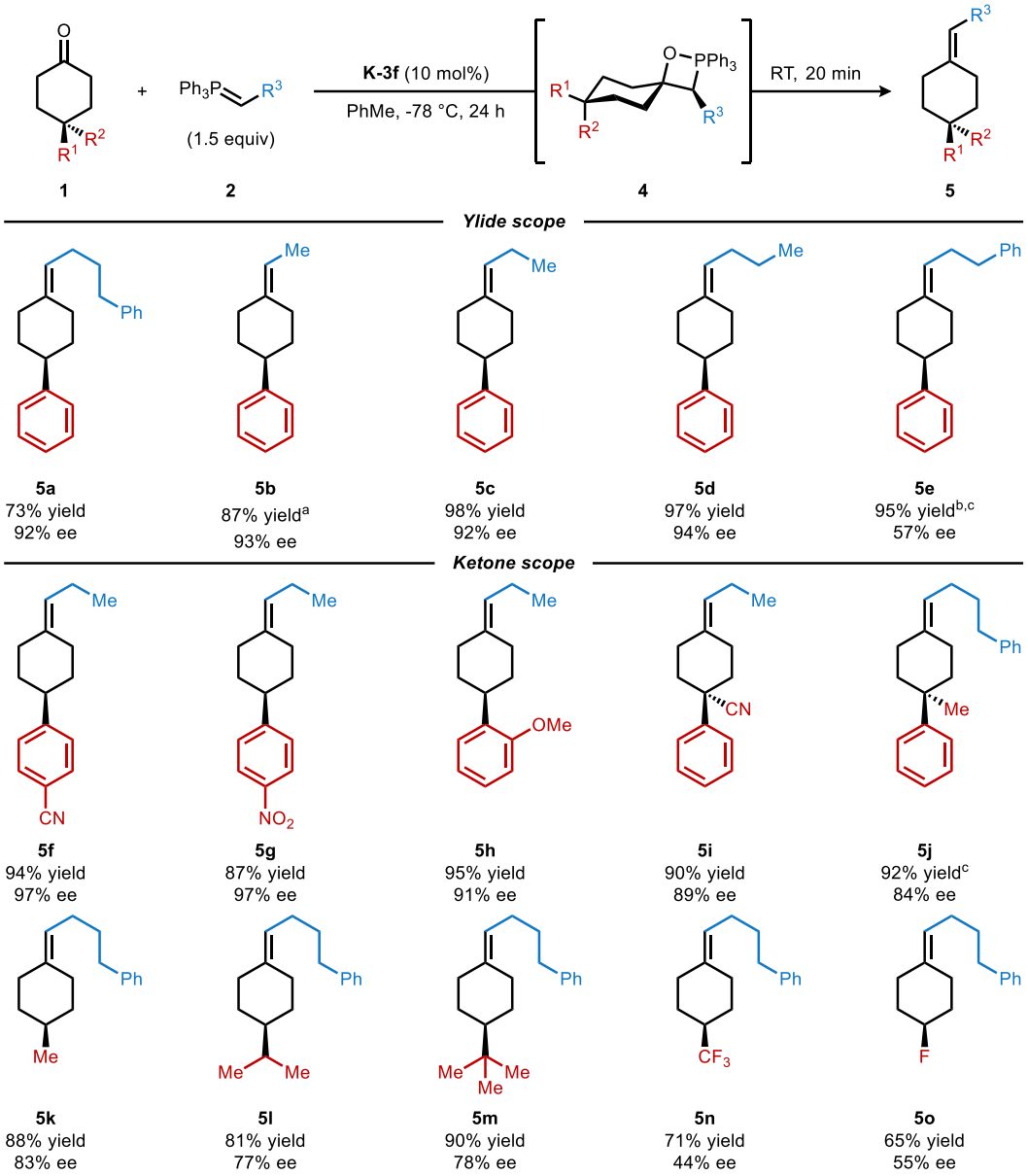

Figure 2. Substrate scope. All reactions were performed on 0.1 mmol scale. Yields correspond to isolated yields of purified products. See Supporting Information for details on the assignment of absolute configuration. [a]Reaction time 4 hours. [b]Reaction time 48 hours. [c]NMR yield.

buffering of Lewis acidity in the two proposed amide-metal-boronate chelates. The low enantioselectivities obtained with catalysts **K-*epi*-3a–f** (Table 1) can be attributed to the steric effect of the *syn* α-boryl methyl group, which likely interferes with formation of the amide-K-boronate chelate (Figure 1E).

The scope of enantioselective olefinations catalyzed by **K-3f** was examined with a set of representative cyclohexanone and ylide substrate combinations (Figure 2). Reactions proceeded effectively with ylide derivatives bearing linear alkyl substituents, with the targeted products generated in high yields and generally high enantioselectivities (**5a–d**). A particular sensitivity to the steric properties of the ylide was noted, as evidenced by a dramatic decrease in ee observed with a β-phenyl derivative (compare **5a** with **5e**). Cyclohexanone derivatives bearing a variety of C4 aryl substituents (**5f–h**) underwent olefination with excellent levels of enantioselectivity, with only slightly lower selectivities obtained for 4,4-disubstituted derivatives (**5i**, **5j**). Reactions with C4 alkyl-substituted derivatives were slightly less enantioselective, with a relatively minor effect associated with substituent steric variation (77-83% ee, **5k–m**).

We sought to glean insight into the basis for the intriguing transannular electronic effects on ee revealed in the substrate scope study (compare **5c** with **5f**). Through-space electric-field effects have been documented previously in hydride additions to 4-substituted cyclohexanones.[41] Computed free energy of activation barriers for the uncatalyzed olefination of a series of *para*-substituted 4-arylcyclohexanones were found to correlate well with the calculated electric field intensity along the forming C–C bond in an equatorial addition of the ylide (Figure 3A). An examination of the **K-3f**–catalyzed olefinations of the same

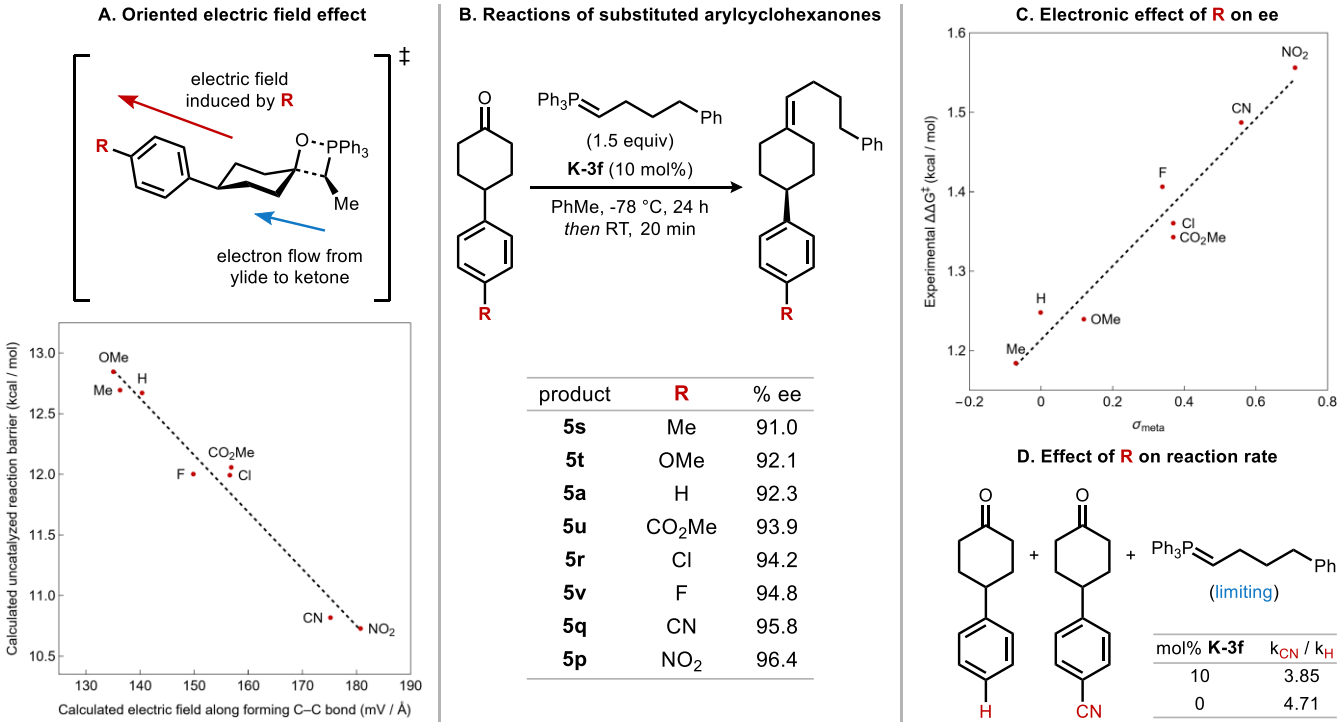

product	R	% ee
5s	Me	91.0
5t	OMe	92.1
5a	H	92.3
5u	CO_2Me	93.9
5r	Cl	94.2
5v	F	94.8
5q	CN	95.8
5p	NO_2	96.4

mol% **K-3f**	k_{CN} / k_H
10	3.85
0	4.71

Figure 3. (A) (top) Proposed model of electric field–induced rate acceleration; (bottom) Computed electric field intensity along the reaction axis correlates with computed rates of olefination for *para*-substituted 4-phenylcyclohexanones. (B) Model reactions performed to study the effect of arylcyclohexanone substitution on ee. (C) Correlation between experimental enantioselectivities and the σ_{meta} parameter for **R**. (D) One-pot competition experiments reveal faster rates in both the catalyzed and uncatalyzed reaction for the more enantioselective substrate.

set of substituted 4-arylcyclohexanones (Figure 3B) revealed that higher enantioselectivity was obtained with substrates bearing more electron-deficient aromatic rings. The enantioselectivity data, expressed as $\Delta\Delta G^{‡}$ (= –RTln(enantiomer ratio)), was plotted against several different standard parameters and found to correlate best with σ_{meta} (Figure 3C, see SI for correlations with other parameters).[42,43] A significant effect on rate was also observed, with electron-withdrawing 4-substituents leading to faster reactions in both the catalyzed and uncatalyzed olefinations (Figure 3D).

A full kinetic analysis of the olefination of ketone **1a** was performed with data collected by UV-visible spectroscopy, monitoring the disappearance of the intensely orange-red ylide **2d** at 520 nm (Figure 4). Plots of the concentration versus time data in a pair of "same excess" experiments with different initial concentrations (Figure 4A, black and red traces) revealed poor graphical overlay, consistent with a catalyst deactivation process.[44] This deactivation could be ascribed directly to product inhibition of **K-3f** by OPA **4d**, as excellent overlay was obtained by addition of the appropriate amount of racemic OPA **4d** to the reaction with lower initial concentrations (Figure 4A, blue trace). A set of "different excess" experiments (Figure 4B) revealed approximate doubling of reaction rate with a doubling of initial ylide concentration, but only a small increase in rate with a doubling of initial ketone concentration. These observations are most consistent with a first-order kinetic dependence on ylide and saturation kinetics in ketone. Variation of the total catalyst concentration $[\mathbf{K\text{-}3f}]_T$ revealed a first-order kinetic dependence (Figure 4C), which in combination with the absence of a nonlinear effect (Figure 4D) is consistent with a monomeric catalyst species throughout the catalytic cycle.

These kinetic results lead us to postulate the catalytic cycle shown in Figure 4E, in which free catalyst **K-3f** reversibly binds ketone **1a** to form complex **A**, followed by turnover-limiting and enantiodetermining irreversible addition of ylide **2d** to form betaine complex **B**, which reversibly dissociates the OPA product **4d** to return free **K-3f**. Consistent with the proposed inhibition of **K-3f** via reversible P–O bond cleavage of **4d** to form **B**, cleavage of OPA intermediates by LiBr to form lithium betaine species has been demonstrated to be facile at –78 °C.[29] On the basis of the kinetic data, it can be estimated that **K-3f** exhibits a threefold preference for binding of OPA **4d** over ketone **1a**. This would induce a shift in catalyst resting state over the course of the reaction from the ketone complex **A** to the betaine complex **B**, manifesting as a roughly zero-order kinetic dependence on ketone in the early stages of the reaction that develops into a first-order dependence as the reaction progresses.

DFT calculations of the putative catalyzed enantiodetermining transition states leading to product **5b** with the 1:1:1 catalyst:ketone:ylide stoichiometry supported by the kinetic analysis reproduced both the correct sense and magnitude of enantioinduction (Figure 4G). The reaction proceeds via a polar 1,2-addition to forge the C–C bond and afford an intermediate potassium betaine

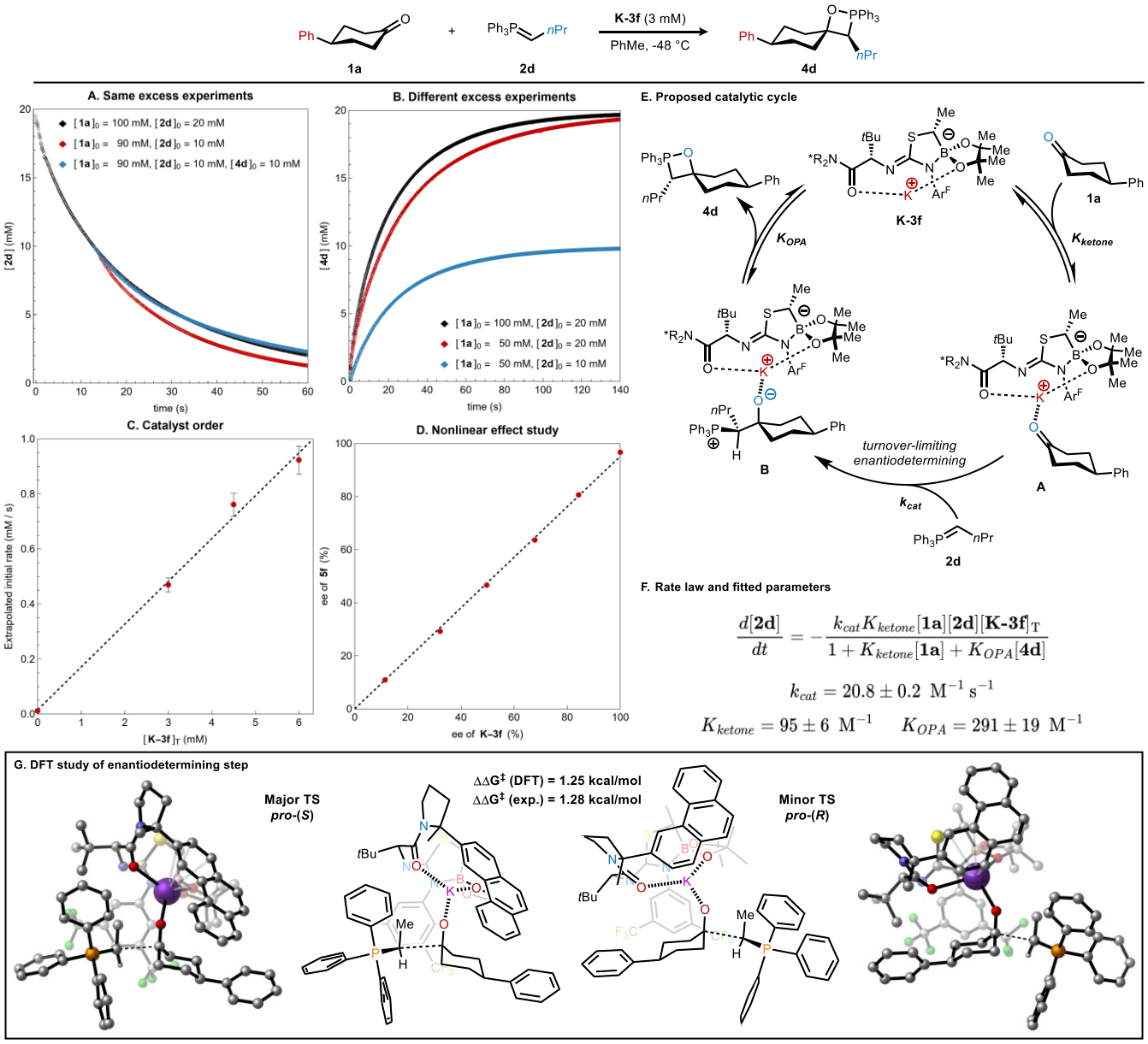

$$\frac{d[\mathbf{2d}]}{dt} = -\frac{k_{cat}K_{ketone}[\mathbf{1a}][\mathbf{2d}][\mathbf{K\text{-}3f}]_T}{1 + K_{ketone}[\mathbf{1a}] + K_{OPA}[\mathbf{4d}]}$$

$$k_{cat} = 20.8 \pm 0.2\ \mathrm{M^{-1}\,s^{-1}}$$

$$K_{ketone} = 95 \pm 6\ \mathrm{M^{-1}} \qquad K_{OPA} = 291 \pm 19\ \mathrm{M^{-1}}$$

Figure 4. Kinetic studies and computational analysis of **K-3f**–catalyzed olefination. (A) Same-excess experiments revealing evidence for inhibition by the OPA product. (B) Different-excess experiments consistent with first-order kinetic dependence on [ylide] and a shift from zero-order to positive-order dependence on [ketone] over the course of the reaction. (C) First-order kinetic dependence on $[\mathbf{K\text{-}3f}]_T$. (D) Absence of nonlinear effect. (E) Proposed catalytic cycle. (F) Proposed rate law and fitted kinetic parameters. (G) Computational analysis of enantiodetermining step reproduces experimental selectivity.

complex.[34] Overall transition state geometry appears to be dictated primarily by two factors: (1) facial selectivity for equatorial addition to the cyclohexanone, and (2) minimization of steric interactions between the triphenylphosphonium moiety and the catalyst framework, dictating the orientation of the ylide substituent. Bulky ylide substituents may hinder steric differentiation with the triphenylphosphonium moiety, leading to lower enantioselectivity (Figure 2, **5e**). While this computational model recapitulates the observed enantioselectivity in the formation of **5b**, the exact basis for enantioinduction is complex and not fully elucidated at this stage.

In summary, highly enantioselective Wittig olefinations of 4-substituted cyclohexanones are catalyzed by a chiral Lewis-acidic potassium-isothiourea-boronate complex possessing a novel macrocyclic chelate structure. The enantiodetermining cycloaddition is a stepwise process involving irreversible polar 1,2-addition to form a potassium betaine complex followed by a reversible cyclization. Future studies will focus on application of the mechanistic observations made here to enantioselective catalysis of other challenging alkali-metal–mediated transformations.

ASSOCIATED CONTENT

Supporting Information

The Supporting Information is available free of charge at http://pubs.acs.org.

Experimental procedures and characterization data for catalyst syntheses, procedures and analytical data for enantioselective reactions, procedures and details of mechanistic studies, and computational studies (PDF)

Crystallographic data for **3f** (CIF)

Crystallographic data for **K-3f·THF** (CIF)

Processed kinetic data (ZIP)

AUTHOR INFORMATION

Corresponding Author

Eric N. Jacobsen – *Department of Chemistry and Chemical Biology, Harvard University, Cambridge, Massachusetts 02138, United States*; orcid.org/0000-0001-7952-3661; Email: jacobsen@chemistry.harvard.edu

Author

Jake Z. Essman – *Department of Chemistry and Chemical Biology, Harvard University, Cambridge, Massachusetts 02138, United States*; orcid.org/0000-0003-2000-2196

Notes

The authors declare no competing financial interest.

ACKNOWLEDGMENT

Financial support for this work was provided by the NIH through GM043214 and GM149244. We thank Dr. Shao-Liang Zheng for X-ray data collection and structure determination. Financial support for the X-ray facility was provided by the Major Research Instrumentation Program under NSF award number 2216066. We thank Prof. Donna Blackmond, Dr. Kurtis Carsch, Dr. Katherine Forbes, Prof. Mark Levin, Dr. Hayden Sharma, and Jonathan Wong for helpful discussions.

REFERENCES

(1) Wittig, G.; Geissler, G. Zur Reaktionsweise Des Pentaphenyl-Phosphors Und Einiger Derivate. *Justus Liebigs Ann. Chem.* **1953**, *580* (1), 44–57. https://doi.org/10.1002/jlac.19535800107.

(2) Wittig, G.; Schöllkopf, U. Über Triphenyl-phosphin-methylene als olefinbildende Reagenzien (I. Mitteil. *Chem. Ber.* **1954**, *87* (9), 1318–1330. https://doi.org/10.1002/cber.19540870919.

(3) Nicolaou, K. C.; Härter, M. W.; Gunzner, J. L.; Nadin, A. The Wittig and Related Reactions in Natural Product Synthesis. *Liebigs Ann.* **1997**, *1997* (7), 1283–1301. https://doi.org/10.1002/jlac.199719970704.

(4) Heravi, M. M.; Zadsirjan, V.; Hamidi, H.; Daraie, M.; Momeni, T. Chapter Three - Recent Applications of the Wittig Reaction in Alkaloid Synthesis. In *The Alkaloids: Chemistry and Biology*; Knölker, H.-J., Ed.; The Alkaloids; Academic Press, 2020; Vol. 84, pp 201–334. https://doi.org/10.1016/bs.alkal.2020.02.002.

(5) Heravi, M. M.; Ghanbarian, M.; Zadsirjan, V.; Alimadadi Jani, B. Recent Advances in the Applications of Wittig Reaction in the Total Synthesis of Natural Products Containing Lactone, Pyrone, and Lactam as a Scaffold. *Monatshefte Für Chem. - Chem. Mon.* **2019**, *150* (8), 1365–1407. https://doi.org/10.1007/s00706-019-02465-9.

(6) Rocha, D. H. A.; Pinto, D. C. G. A.; Silva, A. M. S. Applications of the Wittig Reaction on the Synthesis of Natural and Natural-Analogue Heterocyclic Compounds. *Eur. J. Org. Chem.* **2018**, *2018* (20–21), 2443–2457. https://doi.org/10.1002/ejoc.201800523.

(7) Pommer, H. The Wittig Reaction in Industrial Practice. *Angew. Chem. Int. Ed. Engl.* **1977**, *16* (7), 423–429. https://doi.org/10.1002/anie.197704233.

(8) Wang, Z.-L.; Xu, Y.-H. Progress on the Enantioselective Synthesis of Axially Chiral Cycloalkylidenes. *Synthesis* **2023**. https://doi.org/10.1055/a-2159-1688.

(9) Li, S.; Xu, J.-L.; Xu, Y.-H. Copper-Catalyzed Enantioselective Hydrosilylation of Allenes to Access Axially Chiral (Cyclohexylidene)Ethyl Silanes. *Org. Lett.* **2022**, *24* (32), 6054–6059. https://doi.org/10.1021/acs.orglett.2c02359.

(10) Ma, C.; Sun, Y.; Liu, S.; Li, Z.-M.; Yang, J.; Guo, H.; Zhang, J. Enantioselective Construction of Axially Chiral Cyclohexylidene Scaffolds via Pd-Catalyzed Asymmetric Coupling Reaction. *Chem Catal.* **2022**, *2* (11), 3196–3206. https://doi.org/10.1016/j.checat.2022.09.025.

(11) Crotti, S.; Di Iorio, N.; Artusi, C.; Mazzanti, A.; Righi, P.; Bencivenni, G. Direct Access to Alkylideneoxindoles via Axially Enantioselective Knoevenagel Condensation. *Org. Lett.* **2019**, *21* (9), 3013–3017. https://doi.org/10.1021/acs.orglett.9b00505.

(12) Nimmagadda, S. K.; Mallojjala, S. C.; Woztas, L.; Wheeler, S. E.; Antilla, J. C. Enantioselective Synthesis of Chiral Oxime Ethers: Desymmetrization and Dynamic Kinetic Resolution of Substituted Cyclohexanones. *Angew. Chem. Int. Ed.* **2017**, *56* (9), 2454–2458. https://doi.org/10.1002/anie.201611602.

(13) Xu, P.; Zhou, F.; Zhu, L.; Zhou, J. Catalytic Desymmetrization Reactions to Synthesize All-Carbon Quaternary Stereocentres. *Nat. Synth.* **2023**, *2* (11), 1020–1036. https://doi.org/10.1038/s44160-023-00406-3.

(14) Rein, T.; Pedersen, T. M. Asymmetric Wittig Type Reactions. *Synthesis* **2002**, *2002* (5), 579–594. https://doi.org/10.1055/s-2002-23535.

(15) Tömösközi, I.; Bestmann, H. J. Partielle Asymetrische Synthese Und Absolute Konfiguration von Allencarbonsauren. *Tetrahedron Lett.* **1964**, *5* (20), 1293–1295. https://doi.org/10.1016/S0040-4039(00)90468-4.

(16) Hanessian, S.; Delorme, D.; Beaudoin, S.; Leblanc, Y. Design and Reactivity of Topologically Unique, Chiral Phosphonamides. Remarkable Diastereofacial Selectivity in Asymmetric Olefination and Alkylation. *J. Am. Chem. Soc.* **1984**, *106* (19), 5754–5756. https://doi.org/10.1021/ja00331a070.

(17) Denmark, S. E.; Chen, C. T. Electrophilic Activation of the Horner-Wadsworth-Emmons-Wittig Reaction: Highly Selective Synthesis of Dissymmetric Olefins. *J. Am. Chem. Soc.* **1992**, *114* (26), 10674–10676. https://doi.org/10.1021/ja00052a094.

(18) Kumamoto, T.; Koga, K. Enantioselective Horner-Wadsworth-Emmons Reaction Using Chiral Lithium 2-Aminoalkoxides. *Chem. Pharm. Bull. (Tokyo)* **1997**, *45* (4), 753–755. https://doi.org/10.1248/cpb.45.753.

(19) Mizuno, M.; Fujii, K.; Tomioka, K. The Asymmetric Horner–Wadsworth–Emmons Reaction Mediated by An External Chiral Ligand. *Angew. Chem. Int. Ed.* **1998**, *37* (4), 515–517. https://doi.org/10.1002/(SICI)1521-3773(19980302)37:4<515::AID-ANIE515>3.0.CO;2-Q.

(20) Bestmann, H. J.; Lienert, J. PARTIAL ACID-CATALYTIC ASYMMETRICAL SYNTHESIS OF 4-SUBSTITUTED CYCLOHEXYLIDE ACETIC ACID. 1. *Chem.-Ztg.* **1970**, *94* (13), 487.

(21) Arai, S.; Hamaguchi, S.; Shioiri, T. Catalytic Asymmetric Horner-Wadsworth-Emmons Reaction under Phase-Transfer-Catalyzed Conditions. *Tetrahedron Lett.* **1998**, *39* (19), 2997–3000. https://doi.org/10.1016/S0040-4039(98)00442-0.

(22) Gramigna, L.; Duce, S.; Filippini, G.; Fochi, M.; Franchini, M. C.; Bernardi, L. Organocatalytic Asymmetric Wittig Reactions: Generation of Enantioenriched Axially Chiral Olefins Breaking a Symmetry Plane. *Synlett* **2011**, *2011*

(18), 2745–2749. https://doi.org/10.1055/s-0031-1289516.
(23) Werner, T.; Hoffmann, M.; Deshmukh, S. First Enantioselective Catalytic Wittig Reaction. *Eur. J. Org. Chem.* **2014**, *2014* (30), 6630–6633. https://doi.org/10.1002/ejoc.201402941.
(24) Vedejs, E.; Peterson, M. J. Stereochemistry and Mechanism in the Wittig Reaction. In *Topics in Stereochemistry*; John Wiley & Sons, Ltd, 1994; pp 1–157. https://doi.org/10.1002/9780470147306.ch1.
(25) Byrne, P. A.; Gilheany, D. G. The Modern Interpretation of the Wittig Reaction Mechanism. *Chem. Soc. Rev.* **2013**, *42* (16), 6670–6696. https://doi.org/10.1039/C3CS60105F.
(26) Byrne, P. A.; Gilheany, D. G. Unequivocal Experimental Evidence for a Unified Lithium Salt-Free Wittig Reaction Mechanism for All Phosphonium Ylide Types: Reactions with β-Heteroatom-Substituted Aldehydes Are Consistently Selective for Cis-Oxaphosphetane-Derived Products. *J. Am. Chem. Soc.* **2012**, *134* (22), 9225–9239. https://doi.org/10.1021/ja300943z.
(27) Robiette, R.; Richardson, J.; Aggarwal, V. K.; Harvey, J. N. Reactivity and Selectivity in the Wittig Reaction: A Computational Study. *J. Am. Chem. Soc.* **2006**, *128* (7), 2394–2409. https://doi.org/10.1021/ja056650q.
(28) Vedejs, E.; Marth, C. F. Mechanism of Wittig Reaction: Evidence against Betaine Intermediates. *J. Am. Chem. Soc.* **1990**, *112* (10), 3905–3909. https://doi.org/10.1021/ja00166a026.
(29) Vedejs, E.; Meier, G. P.; Snoble, K. A. J. Low-Temperature Characterization of the Intermediates in the Wittig Reaction. *J. Am. Chem. Soc.* **1981**, *103* (10), 2823–2831. https://doi.org/10.1021/ja00400a055.
(30) Neumann, R. A.; Berger, S. Observation of a Betaine Lithium Salt Adduct During the Course of a Wittig Reaction. *Eur. J. Org. Chem.* **1998**, *1998* (6), 1085–1087. https://doi.org/10.1002/(SICI)1099-0690(199806)1998:6<1085::AID-EJOC1085>3.0.CO;2-G.
(31) Ionkin, A. S.; Marshall, W. J.; Fish, B. M.; Schiffhauer, M. F.; Davidson, F. A Stabilized β-Oxaphosphoniumbetaine: An Elusive Zwitterion. *J. Am. Chem. Soc.* **2007**, *129* (29), 9210–9215. https://doi.org/10.1021/ja071644a.
(32) Uchiyama, Y.; Yamagishi, S.; Yasukawa, T. Observation and Stereochemistry of Betaine Intermediates in the Reaction of Phosphonium Ylide Containing a Phosphaboratatriptycene Skeleton with Benzaldehyde. *J. Org. Chem.* **2022**, *87* (23), 15899–15913. https://doi.org/10.1021/acs.joc.2c02021.
(33) Reitz, A. B.; Nortey, S. O.; Jordan, A. D.; Mutter, M. S.; Maryanoff, B. E. Dramatic Concentration Dependence of Stereochemistry in the Wittig Reaction. Examination of the Lithium Salt Effect. *J. Org. Chem.* **1986**, *51* (17), 3302–3308. https://doi.org/10.1021/jo00367a010.
(34) McEwen, W. E.; Beaver, B. D. ROLE OF THROUGH-SPACE 2p–3d OVERLAP EFFECTS IN LITHIUM-ION CATALYZED WITTIG REACTIONS. *Phosphorus Sulfur Relat. Elem.* **1985**, *24* (3), 259–271. https://doi.org/10.1080/03086648508074237.
(35) Hooper, D. L.; Garagan, S.; Kayser, M. M. Lithium Cation-Catalyzed Wittig Reactions. *J. Org. Chem.* **1994**, *59* (5), 1126–1128. https://doi.org/10.1021/jo00084a034.
(36) Sharma, H. A.; Essman, J. Z.; Jacobsen, E. N. Enantioselective Catalytic 1,2-Boronate Rearrangements. *Science* **2021**, *374* (6568), 752–757. https://doi.org/10.1126/science.abm0386.
(37) Essman, J. Z.; Sharma, H. A.; Jacobsen, E. N. Development of Enantioselective Lithium-Isothiourea-Boronate–Catalyzed Matteson Homologations. *Synlett* **2023**, *34*, 2061–2070. https://doi.org/10.1055/a-2099-6557.
(38) Mayer, U.; Gutmann, V.; Gerger, W. The Acceptor Number — A Quantitative Empirical Parameter for the Electrophilic Properties of Solvents. *Monatshefte Für Chem. Chem. Mon.* **1975**, *106* (6), 1235–1257. https://doi.org/10.1007/BF00913599.
(39) Beckett, M. A.; Strickland, G. C.; Holland, J. R.; Sukumar Varma, K. A Convenient n.m.r. Method for the Measurement of Lewis Acidity at Boron Centres: Correlation of Reaction Rates of Lewis Acid Initiated Epoxide Polymerizations with Lewis Acidity. *Polymer* **1996**, *37* (20), 4629–4631. https://doi.org/10.1016/0032-3861(96)00323-0.
(40) Wittig reactions with stabilized and semi-stabilized ylides are well established to proceed only under conditions where the OPA decomposes rapidly to the alkene + phosphine oxide. For a detailed discussion, see ref. 25.
(41) Kwart, Harold.; Takeshita, T. Evidence for Parallel Control of Reaction Rate and Stereochemistry via the Electrostatic Influence of Remote Substituent Dipoles. *J. Am. Chem. Soc.* **1962**, *84* (14), 2833–2835. https://doi.org/10.1021/ja00873a043.
(42) Wheeler, S. E.; Houk, K. N. Substituent Effects in the Benzene Dimer Are Due to Direct Interactions of the Substituents with the Unsubstituted Benzene. *J. Am. Chem. Soc.* **2008**, *130* (33), 10854–10855. https://doi.org/10.1021/ja802849j.
(43) Wheeler, S. E.; Houk, K. N. Origin of Substituent Effects in Edge-to-Face Aryl-Aryl Interactions. *Mol. Phys.* **2009**, *107* (8–12), 749–760. https://doi.org/10.1080/00268970802537614.
(44) Blackmond, D. G. Kinetic Profiling of Catalytic Organic Reactions as a Mechanistic Tool. *J. Am. Chem. Soc.* **2015**, *137* (34), 10852–10866. https://doi.org/10.1021/jacs.5b05841.

For Table of Contents Only